IEEE Access
Multidisciplinary | Rapid Review | Open Access Journal

Received 29 August 2022, accepted 12 September 2022, date of publication 16 September 2022,
date of current version 30 September 2022.

Digital Object Identifier 10.1109/ACCESS.2022.3207475

RESEARCH ARTICLE

All-Optical Distributed MIMO for LiFi: Spatial Diversity Versus Spatial Multiplexing

SEPIDEH MOHAMMADI KOUHINI, (Graduate Student Member, IEEE), JULIAN HOHMANN, SREELAL MAVANCHERY MANA, PETER HELLWIG, DOMINIC SCHULZ, ANAGNOSTIS PARASKEVOPOULOS, (Member, IEEE), RONALD FREUND, (Member, IEEE), AND VOLKER JUNGNICKEL, (Member, IEEE)
Photonic Networks and Systems, Fraunhofer Heinrich Hertz Institute, 10587 Berlin, Germany

Corresponding author: Sepideh Mohammadi Kouhini (sepideh.kouhini@hhi.fraunhofer.de)

This work was supported in part by the European Union's Horizon 2020 Marie Skłodowska-Curie International Training Network VisIoN under Grant 764461, and in part by the EU Horizon 2020 Innovation Action ELIoT under Grant 825651.

ABSTRACT LiFi or networked optical wireless communication is likely to play an important role in offloading mobile data traffic from radio into the optical spectrum. As the number of Internet of Things (IoT) devices is growing, the RF spectrum becomes a rare resource. Imaging IoT sensors like cameras, ultrasonic devices, and Lidars have real-time requirements, need a high-capacity uplink, and operate in environments that cause or are sensitive against electromagnetic interference. In this paper, for the first time, we present realtime communication over an all-optical fixed-wireless LiFi link based on the distributed multiple-input multiple-output concept. For distributing the wireless signals, plastic optical fibers are used as an analog front-haul. We study the operation of the distributed multiple-input multiple-output link in two modes, i.e., spatial diversity and spatial multiplexing. For the diversity mode, a new combiner is presented, which can support equal gain as well as selection combining. We demonstrate that selection combining is highly effective and enables a similar LiFi performance in up- and downlink, as it is desirable for industrial applications. For the spatial multiplexing mode, we observe that the channel rank and the achievable throughput depend strongly on the user location. As effective solutions, we study the benefits of angular diversity and multiple-input multiple-output mode switching together with multi-user multiplexing and conclude that a dynamic switching between spatial diversity and spatial multiplexing is a practical approach.

INDEX TERMS Optical wireless communication, plastic optical fiber, multi-user, multiple-input-multiple-output, diversity, spatial multiplexing.

I. INTRODUCTION

LiFi denoted as light fidelity is a networked short-range optical wireless communication (OWC) technology using light instead of radio waves as the wireless medium. In indoor environments, LiFi offers a practical solution, where additional spectrum is needed. It is evident to complement mobile radio with LiFi by offloading the wireless traffic from radio into the optical spectrum [1], [2]. Moreover, light does not penetrate through walls and it is robust against electromagnetic interference and jamming [3]. LiFi is based on a network of small cells, with only a few users per cell. This enables frequent reuse of the optical spectrum, due to the confinement of optical wave propagation inside the light beam. Distributed multiple-input multiple-output (D-MIMO) is a modern wireless communication approach enabling seamless mobility between distributed optical frontends that are deployed as wireless infrastructure [4]. This approach can support a higher network capacity, as well as lower latency. Here mobility is supported by implementing MIMO algorithms at the lower physical and medium access layers in the protocol stack, whereas conventional mobile networks

The associate editor coordinating the review of this manuscript and approving it for publication was Liang Yang.

implement those at the transport and higher layers [5]. This advanced approach aims at new services in the future Industrial Internet-of-Things (IIoT), where wired communication links will be replaced by wireless connections that, however, interfere with each other. IIoT applications can be divided into monitoring and machine-to-machine (M2M) communication via wireless infrastructure. For monitoring, machines collect small data packets e.g., device position, device identifier, and a time stamp. Human interaction is very limited or not necessary. Therefore, the reliability of the communication link is crucial. By means of M2M communication, machines interact with each other to accomplish a complex task. Delays or any malfunction of the system would lead to high risk for production and human safety. Therefore, future IIoT requires very reliable communication links. Moreover, the number of IoT devices connected to the cloud is estimated to reach 10 devices per square meter [6]. Future IIoT devices are expected to relay data from a giant number of sensors to the cloud, in order to allow for artificial intelligence (AI) based decisions in real-time.

While 4G cellular radio uses frequencies at few GHz, it is expected that 5G will cover higher frequencies up to 75 GHz. For 6G, even higher frequencies in the sub-Terahertz and optical spectrum are considered. Optical components are well established in various applications and available in the mass market. Using the light, as OWC, also known as visible light communication (VLC) and LiFi is increasingly investigated for communication integrated with positioning. Moreover, first standards like G.vlc, IEEE 802.15.13, and 802.11bb become available as signs of growing technology readiness.

On the other hand, as OWC connections mostly rely on the line-of-sight (LOS), which can be occasionally blocked. Therefore, an additional technique is required to enhance the reliability of the wireless links. Multiple-input multiple-output (MIMO) is a well-known tool to enhance the reliability additionally the capacity of communication in the radio frequency (RF) domain [7]. These advantages of MIMO can also be used for OWC [8]. In [9] and [10], the potential of using multiple networked LiFi access points (AP)s for enhanced robustness against blockage has been demonstrated in real industry and hospital application scenarios. Among the various MIMO schemes, spatial diversity (SDIV) or repetition coding (RC), spatial modulation (SM) and spatial multiplexing (SMUX) have been proposed for OWC [11], [12].

In [13], the inherent redundancy of SDIV is considered as the potential tool to enhance the robustness against blockage and shadowing for OWC. Theoretical and experimental evaluation of SDIV verified the enhanced robustness in a real indoor environment in [14] and [15]. For higher data rate in case of having unequal channel gain, SM is incorporated with SDIV. SM encodes data in the spatial domain by activating a single transmitter in a MIMO link while the rest of the transmitters remain idle [16], [17]. In [18], this technique has been combined with orthogonal frequency-division multiplexing (OFDM) for robust performance in Rician fading channels.

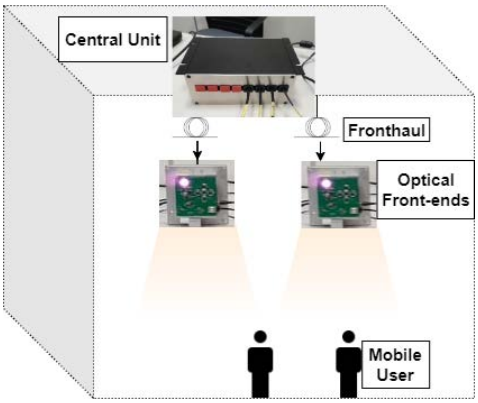

FIGURE 1. Topology of distributed MIMO link setup for LiFi in an indoor scenario.

However, since only one transmitter is active at a particular instant, spectral efficiency is limited.

Another method for increasing the capacity and spectral efficiency is the SMUX technique, where independent data streams are transmitted in parallel. The SMUX benefits from inter-channel-interference (ICI). In [19], the authors proposed a generalized SMUX technique by activating variable numbers of LEDs to transmit multiple data streams. The authors in [20] proposed a signal space diversity scheme incorporated with SM for a 2×1 OWC MISO system. The results showed that an adaptive MIMO is required for an OWC system. In addition, performance evaluation has been presented using a multi-directional receiver with different MIMO techniques in [21]. Both studies rely on bit-error-rate (BER) and signal-to-noise ratio (SNR) as figures of merit. The authors in [20] show that the RC is superior to SM, while SMUX was not considered. The authors of [21] look at a large scale scenario, which is interference-limited, in the SMUX mode at least. The evaluation framework of [21] uses the required SNR to reach a given BER, while we are using the achievable throughput, which is considered more practical. The angular diversity (AD) is shown to require less SNR in [21], and reaches higher throughput in our work, compared to not using it. Qualitatively, these results are consistent. Note that [20] and [21] are based on simulation, while our work is based on measurement in real-time. So far, the impacts of using SDIV and SMUX have not been thoroughly investigated yet.

This paper investigates the application of distributed MIMO for LiFi in the proposed system architecture, which is composed of a wired fronthaul followed by distributed wireless links, as shown in Fig. 1. Our first objective is to develop a mathematical model of the distributed MIMO link by using concatenated wired and wireless links, where either SDIV or SMUX can be used. Next, we evaluate each method to enable robust high-speed communication over the LiFi link. Our second objective is to assess the proposed setup through simulations and experiments to obtain quantitative results. In the performance analysis, SNR versus frequency and the achievable throughput are used as figures of merit.

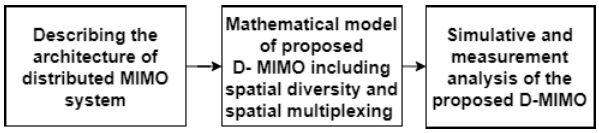

FIGURE 2. Methodology of the article.

Preliminary results of the present study were published in [22] and [23]. In this paper, we extend our study and provide the following main contributions:

- A mathematical framework for distributed optical wireless MIMO links using POF as an analog fronthaul
- Extension for both down- and up-link including various diversity combining techniques
- A simulation-based and experimental study of a 4×2 MIMO cell with spatial diversity
- A first POF combiner including both equal gain combining (EGC) and selection combining (SC)
- A mobile device architecture that includes AD
- Performance results in a real-time LiFi link for a 2×4 LiFi cell.

The methodology of this article is illustrated in Fig. 2. The remainder of this paper is organized as follows. Section II introduces the proposed distributed MIMO topology. Section III presents the mathematical model of the distributed MIMO link. Sections IV and V report the evaluation framework and our results, respectively. Finally, the main conclusions of this paper are presented in section VI.

II. DISTRIBUTED MIMO FOR LiFi

Distributing wireless APs is a well-known approach in cellular radio networks to extend coverage and increase capacity. The idea behind is frequency reuse, i.e. distant APs can reuse the same spectrum [24]. However, the capacity is limited by interference, when the nearer AP reuses the spectrum. In MIMO systems, the capacity is high if the channel vectors of mobile users (MUs) are orthogonal to each other. Each channel vector contains all links between multiple APs and one MU. In radio links, this is likely because indoor radio propagation is dominated by non-LOS signals. Light propagation is mostly based on the LOS. The idea of D-MIMO is to deploy multiple APs e.g. in a regular grid at the ceiling to serve jointly one or multiple MUs in the service area. When using D-MIMO in LiFi systems, transmitters and receivers should be sufficiently separated from each other, or at least pointed into different directions, if co-located. Due to spatial separation, orthogonality between the channel vectors is then improved.

In [25] it was demonstrated that, by using D-MIMO, the performance is improved and a higher data rate is achievable because the channel matrix is well-conditioned. In [5], [23], [26], and [27], a D-MIMO architecture for LiFi was investigated and its performance evaluated. It uses a coordinator, implemented as a central unit (CU) and multiple APs, also denoted as optical frontends (OFEs). In order to distribute the OFEs, a fixed fronthaul link is required, forwarding the signal from the CU to each OFE. Waveform transmission over the fronthaul can be regarded as relaying, for which Decode-and-forward (DF) as well as amplify-and-forward (AF) are commonly used [25]. In the DF link, the received signal is decoded first, then re-encoded and forwarded to the user [28]. Even though DF is favored by the industry, it is more complex and increases latency. In the AF link, the received signal is amplified and forwarded by the relay. The received signal contains additional noise, which after amplification, can degrade the overall performance. This is particularly important in the uplink, where the received wireless signal can be very weak. To optimize the performance, an automatic gain control (AGC) based on the received signal strength indicator (RSSI) is required. In [29], a practical method for D-MIMO using AF over plastic optical fiber (POF) was presented, where the AGC is co-located with the CU and the attenuation over the POF link is compensated by electrical amplifiers.

Accordingly, as shown in Fig. 1, the distributed MIMO topology contains the following parts:

- Central unit (CU)
- Fronthaul
- Optical front-ends (OFE)
- Mobile user (MU)

In the following, the functionality of each part is elaborated.

A. CENTRAL UNIT

The CU is providing a fundamental channel estimation and feedback protocol with each MU to select the strongest OFE signals, which can be used for joint transmission and reception. Using the so-called Cloud Radio Access Network (C-RAN) with centralized signal processing is a common concept in cellular radio systems [30]. It is currently proposed in the IEEE P802.15.13 standard of LiFi for industrial scenarios.

In this paper, we assume that the selection of the best serving, i.e., nearby OFEs in the CU is already completed and the signals from distant OFEs can be ignored. This assumption is justified by the LOS-based light propagation, which implies that the electrical signal reduces by a path-loss exponent of four, even in indoor environments. [1]

B. FRONTHAUL

In order to transmit LiFi signals from the CU to each OFE, the fronthaul link is used. There are several analog media for distributing the CU signal to each optical frontend, such as twisted-pair, coax cables, power-line communications (PLC), besides plastic optical fiber (POF). The powerline is shared among several power outlets, which creates multipath effects. Moreover, PLC is restricted due to spectrum regulations, as the powerlines also act as an antenna, causing

[1] This is different for radio links, where the path loss exponent in indoor environments is between one and two, typically, due to the dominant non-LOS propagation.

interference to other ambient services, such as FM radio. Coax cables are expensive and, besides satellite television and Internet delivery, hardly used in indoor environments. Twisted-pair cables enable reliable transmission, which is well known for phone lines and Ethernet cables, and have been tested for LiFi [29]. However, proper shielding is needed to avoid unwanted emissions and to make the link robust against electromagnetic interference.

An advantage of electrical media is that powering can be supplied along with the fronthaul. Note that optical frontends for LiFi will be co-located with the illumination infrastructure, so that homogeneous coverage similar to the existing luminaries is achievable. Through the powerlines feeding the luminaries, powering will be available likewise. Hence, only the LiFi waveforms need to be delivered from the CU to each OFE.

Therefore, we propose POF as a practical solution for certain use cases, which are sensitive to electromagnetic interference, such as in an aircraft, in medical and manufacturing environments [29],[2] [9]. Polymethyl methacrylate (PMMA) step index POF known as a standard POF is an attractive solution for the fronthaul of LiFi systems [23]. POF is robust against electromagnetic interference, has a small bending radius, is easy as well as cheap to install, and bridges up to 50 meters link distance. In [23], early results for implementing distributed MIMO in LiFi systems by using POF as an analog fronthaul are shown.

C. OPTICAL FRONT-ENDS

The presented OFEs are ceiling-mounted devices containing four high-power LEDs and five photodiodes. Each photodiode is equipped with a trans-impedance amplifier (TIA) and the electrical outputs of the TIAs are summed up. The OFEs are in charge of providing bi-directional wireless communication between the CU and MUs.

D. MOBILE USER

Current MUs for LiFi are handheld devices, which typically have an OFE pointing upwards for bidirectional wireless communication.

In this paper, we study MUs with one and two OFEs. When one OFE is used, it points upwards. If two OFEs are used, they point upwards. There can be an additional tilt by an angle α (e.g., $\alpha = \pm 45°$). This is also denoted as AD. AD helps provide more than one LOS link to the distributed OFE (D-OFE)s at the ceiling, which is beneficial for the desired robustness against blockage of the LOS and to enhance the coverage. In a D-MIMO link, AD can also enhance the rank of the MIMO channel matrix. Looking into different directions can increase the orthogonality of the channel vectors from all OFEs to one OFE at the MU and, thus, allows the use of parallel communication links between the MU and multiple OFEs in the ceiling infrastructure. The benefits of equipping LiFi MU with AD are outlined in [31] and [32].

[2]While powering could theoretically be provided over the POF, it would not be enough to feed the optical frontend in a LiFi system, which is capable of providing homogeneous coverage in an area of a few square meters.

III. SYSTEM MODEL

In this section, we present the mathematical model of our distributed MIMO link, which is a concatenation of the analog fronthaul over POF and the wireless link [23]. We explain the various MIMO modes of SDIV and SMUX, and how to compute data rates. The model is used for quantitative comparison, and the analysis of experimental results.

A. DISTRIBUTED MIMO MODEL

In this section, the mathematical model for the distributed MIMO link, including the channel matrix H(f), is presented. This model describes the concatenation of POF and wireless links in the frequency domain. The model is parallelized and includes the crosstalk between the parallel wireless signals over the air. In the model, DC-OFDM is used as a modulation scheme. We assume that the CU is connected to N_T OFEs all working at the same optical wavelength. The received signal vector at each MU for the f-th OFDM sub-carrier is described by

$$\mathbf{y}(f) = \mathbf{H}(f)\,\mathbf{x}(f) + \mathbf{n}(f), \tag{1}$$

where $\mathbf{H}(f)$ is the $N_{MU}N_R \times N_T$ end-to-end analog channel matrix, $\mathbf{x}(f)$ is the $N_T \times 1$ transmit signal vector, $N_{MU}N_R \times 1$ with N_{MU} being the number of MUs and N_R their receivers, and $\mathbf{n}(f)$ is the vector of the additive white Gaussian noise with zero-mean and variance $\sigma_n^2 = N_0 B$, where N_0 and B denote the noise power spectral density and the modulation bandwidth, respectively [23]. The power is distributed equally over the subcarriers. The overall channel matrix $\mathbf{H}(f)$ including the wired and wireless channels can be written as a concatenation of two contributions as

$$\mathbf{H}(f) = \mathbf{Z}(f)\mathbf{G}(f), \tag{2}$$

where $\mathbf{Z}(f) \in \mathbb{R}^{N_{MU}N_R \times N_T}$ is the wireless MIMO channel matrix and $\mathbf{G}(f) \in \mathbb{R}^{(N_{PD}=N_T)\times N_T}$ describes the parallel POF fronthaul links. Note that this model can potentially also describe cross-talk in the POF link [23], which is not considered in this paper. The coefficients of $\mathbf{Z}(f)$ are computed as

$$Z_{l,j}(f) = H_{\mathrm{LED}_j}(f) g_{\mathrm{TX}}(\phi_j) g(d_{j,l}) g_{\mathrm{RX}}(\phi_l) H_{\mathrm{PD}_l}(f), \tag{3}$$

where $H_{\mathrm{LED}_j}(f)$ represents the frequency response of the LED plus driver, $g_{\mathrm{TX}}(\phi_j)$ stands for the radiation pattern, $d_{j,l}$ is the distance between j-th D-OFE and the l-th MU, ϕ_j, ϕ_l are the angles of the link between transmitter and receiver, respectively, $g(d_{j,l})$ denotes the path loss in the wireless link, $g_{\mathrm{RX}(\phi_l)}$ and $H_{\mathrm{PD}_l}(f)$ are is the photodiode sensitivity and the frequency response of the photoreciver, respectively [11], [33]. The POF is a color-dependent medium. However, in this paper, we assume that all fronthaul signals are transmitted via separate POF links at the same wavelength and there is no crosstalk between them when distributing the signal

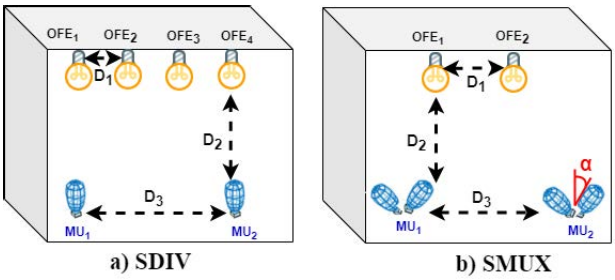

FIGURE 3. Simulation Environment for a) spatial diversity (SDIV), which consists of four OFEs connected in series pattern and two MUs b) Spatial multiplexing (SMUX) setup with two OFEs and two MUs. Each MUs is equipped with two OFEs, which are tilted with angle α.

from the CU to the OFEs. In this case, $\mathbf{G}(f) = G_0\mathbf{I}_{N_T}$ is a diagonal matrix, where G_0 represents the POF channel gain and I_{N_T} is an identity matrix. At the OFEs, the signals are forwarded over the wireless link to the MUs. $H_{l,i}(f)$ represents each individual link from each transmitter i in the ceiling infrastructure to each receiver l at the MU, for $j = 1, \ldots, N_T$, and corresponding j-th OFE LED, which is given by

$$H_{l,i}(f) = \sum_{j}^{N_T} Z_{l,j}(f)G_{j,i}(f), \tag{4}$$

where the sum describes the cross-talk in the wireless channel. It can be removed by MIMO signal processing for the combined MIMO channel given by: $H_{l,i}(f) = Z_{l,i}(f)G_{i,i}(f)$. By cancelling the wireless cross-talk, parallel channels are created over the concatenated POF and wireless links. Next, different models for SDIV and SMUX in the downlink and uplink are presented.

B. SPATIAL DIVERSITY

In SDIV mode, the same data stream is transmitted over multiple transmitters. This approach increases the reliability of the transmission. We distinguish models for downlink and uplink communication for various combining methods. The cell layout of SDIV is a 4×2 MIMO setup as shown in Fig. 3 (a).

1) DOWNLINK

For the downlink, we consider two users $k = 1, 2$. The received signal for user k is expressed as

$$y^{(k)} = \left(h_1^{(k)}\ h_2^{(k)}\ h_3^{(k)}\ h_4^{(k)}\right) \cdot \begin{pmatrix} x_1 \\ x_2 \\ x_3 \\ x_4 \end{pmatrix} + n^{(k)}. \tag{5}$$

The CU signal is repeated over all distributed OFEs, yielding:

$$\vec{x}^{(k)} = \vec{w}.d^{(k)} = \begin{pmatrix} 1 \\ 1 \\ 1 \\ 1 \end{pmatrix} .d^{(k)}. \tag{6}$$

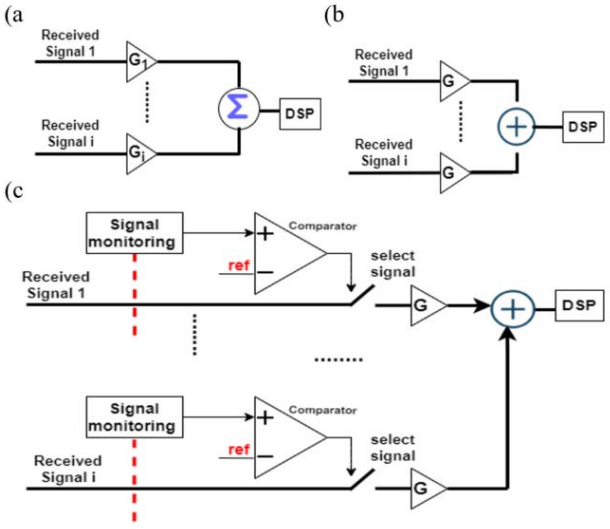

FIGURE 4. Diversity combining was implemented as analog electronics in the combiner unit, (a) maximum ratio combining with different weight factors, (b) equal gain combining, which accumulates the receiving signal with equal gain, (c) selection combining, which monitors the received signal strength and select the strongest ones only.

where the elements of $\vec{w}$ amount all to 1 to indicate the spatial repetition code used and $d^{(k)}$ is the data signal for the $k^{(th)}$ MU.

2) UPLINK

In the uplink, the signal of each MU is received by all OFEs, which is described for one of the users as

$$\begin{pmatrix} y_1 \\ y_2 \\ y_3 \\ y_4 \end{pmatrix} = \begin{pmatrix} h_1 \\ h_2 \\ h_3 \\ h_4 \end{pmatrix} . x + \begin{pmatrix} n_1 \\ n_2 \\ n_3 \\ n_4 \end{pmatrix} . \tag{7}$$

where y_l and n_l are the received signal and the noise at the distributed-OFE $l = 1, \ldots N_T$ and x is the transmitted signal of the one MU. In order to retrieve the transmitted data $\widehat{x}$, we apply a weighted average of all received signals as:

$$\widehat{x} = \begin{pmatrix} w_1 \\ w_2 \\ w_3 \\ w_4 \end{pmatrix} , \vec{y}. \tag{8}$$

where the coefficients w_l depend on the used diversity combining technique. Therefore, maximum ratio combining, equal gain combining and selection combining are investigated.

a: MAXIMUM RATIO COMBINING

Maximum ratio combining (MRC) is considered as optimal linear combining solution in additive white Gaussian noise as shown in Fig. 4 (a). For MRC, each received signal is multiplied by a weighting factor proportional to the channel coefficient (G_{MRC}=$G_1, \ldots, G_i$), and then all the so weighted signals are summed up. In [34] it is shown that

MRC adjusts the weights optimally, compared to other techniques. However, the implementation of MRC in real-time is complex. Measuring the SNR for each received branch typically requires multiple analog-to-digital converters in the baseband processing which then performs MRC using the w_{MRC} defined in (9), where each w_i is given in (10).

$$w_{MRC} = G_{MRC}. \begin{pmatrix} w_1 \\ w_2 \\ w_3 \\ w_4 \end{pmatrix} \tag{9}$$

$$w_i = \frac{h_i}{\sqrt{\sum_{j=1}^{i} |h_j^2|}} \tag{10}$$

b: EQUAL GAIN COMBINING

The EGC technique weights all received signals equally for diversity reception, i.e. $w_i = 1$. Fig. 4 (b) shows the EGC block diagram, with the same gain for all received signals. In this way, estimation of the SNR for all received signals is not required, making the implementation simpler. On the other hand, EGC does not scale well for large numbers of receivers, as the optical wireless channel is spatially selective and many receivers may not add significant useful signal but will increase the noise.

c: SELECTION COMBINING

This technique chooses the received signals with the best SNRs. The process of monitoring and selecting the signal is shown in Fig. 4 (c). At first, the signal power is monitored and only added if it is larger than a pre-defined threshold. In our implementation, the received power is estimated in the first μs when a data packet is received. A fast analog comparator checks the received signal power versus an optimized reference value. If the signal is higher than the threshold, it is included in the combining. For branch $i = 0, .., N_T$ of the received signal, the w_{SC} are defined as

$$w_{SC_i} = G_{SC_i}. \begin{pmatrix} w_1 \\ w_2 \\ w_3 \\ w_4 \end{pmatrix}.$$

$$w_i = \begin{cases} 1 & \text{if } |y_i| \geq y_{threshold} \\ 0 & \text{otherwise.} \end{cases} \tag{11}$$

C. SPATIAL MULTIPLEXING

To increase the channel capacity without additional spectral resources, SMUX is used. Independent data streams are transmitted simultaneously through multiple transmitters. The signal in each receiver branch is a linear combination of multiple data signals from all transmitters [22], [35], [36]. However, detection is more complex than for SDIV. In this paper, we show linear MIMO detection based on zero forcing (ZF) and minimum mean square error (MMSE). Because MMSE is improved compared to ZF, it is used during the measurement.

d: ZERO FORCING

To retrieve the transmitted signal, the left-handed Moore-Penrose pseudo-inverse of the channel matrix H is obtained using a weighting matrix w_{ZF} as $w_{ZF} \times H = I$ to reconstruct the transmitted signal [36] based on following

$$\widehat{x}_{ZF} = w_{ZF}.\vec{y}. \tag{12}$$

The weight matrix can be computed as

$$w_{ZF} = (H^H H)^{-1} H^H. \tag{13}$$

Therefore, the retrieved signal after zero-forcing is obtained as:

$$\widehat{x}_{ZF} = x + w_{ZF}.n, \tag{14}$$

where H^H is the Hermitian transpose of the MIMO channel matrix H and n is the noise vector. The drawback of ZF is the anisotropic noise enhancement, which can degrade the system performance, depending on the properties of the channel matrix H. Accordingly, ZF is suitable when the SNR and the rank of the channel matrix are high.

e: MINIMUM MEAN-SQUARE ERROR

MMSE is also a linear equalizer and uses a modified filtering matrix compared to ZF. The weight matrix for MMSE (w_{MMSE}) can be defined as [36]

$$w_{MMSE} = (H^H H + N_0 I)^{-1} H^H, \tag{15}$$

so that the transmitted signal is retrieved by

$$x_{MMSE} = w_{MMSE} \times y. \tag{16}$$

where N_0 refers to the noise power and I is the identity matrix. This method can overcome some implications of the noise enhancement of ZF for ill-conditioned channel matrices through regularization of the inverse matrix which is achieved through the additional term $N_0 I$ in equation 16 [36].

D. THROUGHPUT EVALUATION

The singular value decomposition (SVD) is an effective mathematical tool for evaluating the MIMO capacity [37], [38]. In this section, we use the SVD and assume that the channel state information is available at the D-OFEs and MUs. The SVD converts the MIMO link into parallel channels, where the maximum number of parallel channels is equal to the minimum number of transmitters and receivers. At the f-th subcarrier $H(f)$, the SVD can be written as

$$\mathbf{H}(f) = \mathbf{U}(f)\mathbf{D}(f)\mathbf{V}(f)^H, \tag{17}$$

where U and V are unitary matrices and D is a matrix, which contains the singular values on the main diagonal and zeros elsewhere.

$$\mathbf{U}(f) \in \mathbb{C}^{N_U N_R \times N_U N_R} \tag{18}$$

$$\mathbf{V}(f) \in \mathbb{C}^{N_T \times N_T} \tag{19}$$

$$\mathbf{D}(f) \in \mathbb{R}_{+}^{N_U N_R \times N_T}. \tag{20}$$

TABLE 1. LiFi Cell Layouts, Scenarios and Cases.

SDIV		
Layout	Scenarios	
4 ×2 MIMO	I: D_1= 90cm, D_2= 200cm, D_3=5cm II: D_1= 90cm, D_2= 200cm, D_3= 90cm III: D_1= 90cm, D_2= 200cm, D_3= 270cm	
SMUX		
Layout	Scenarios	Cases
2 ×4 MIMO	I: D_1= 70cm, D_2=100cm, D_3= 5cm II: D_1= 70cm, D_2=100cm, D_3= 70cm III: D_1= 70cm, D_2= 100cm, D_3= 140cm	without angular diversity with angular diversity

Based on [39] and [40], $\lambda_1(f) \geq \lambda_2(f) \geq \ldots \geq \lambda_K(f)$, where $K = \min(N_U N_R, N_T)$ denotes the rank of $\mathbf{H}(f)$. In some kcases, the rank can be reduced, particularly in LOS MIMO channels when transmitters and/or receivers are near to each other. Based on the SVD, we can also compute the achievable throughput following [41], by using the normalized channel matrix defined in [37] and [23]

$$R = \Delta_B \sum_{n=1}^{N} \sum_{k=1}^{K} \log_2 \left(1 + \frac{SNR}{N_T \eta_H \Gamma} \lambda_k^2(f_n)\right), \qquad (21)$$

where SNR indicates signal-to-noise ratio, N the number of subcarriers, ΔB the bandwidth occupied by each subcarrier, η_H the average path loss of $\mathbf{H}(f)$ and $\Gamma = 10$ an empirical scaling factor taking into account the reduced modulation amplitude for the DC-biased OFDM signal at the transmitter to avoid non-linear distortion (clipping of negative signals) as well as imperfect constellation shaping [42].

When serving one user per time slot, the SNR for that user can be estimated as follows

$$SNR^{(k)} = \frac{|h^{(k)}.\vec{w}|^2.|d^{(k)}|^2}{|n|^2}, \qquad (22)$$

where n is the additive white Gaussian noise amplitude.

IV. EVALUATION FRAMEWORK

In this paper, we propose an advanced optical D-MIMO architecture for LiFi and investigate the basic transmission modes for SDIV and SMUX. In the following, our evaluation framework is explained for simulations and measurements.

A. SIMULATION ENVIRONMENT

The simulations have been carried out in Matlab. The physical layer of the ITU-T recommendation G.9991 for LiFi was implemented. As discussed in the mathematical model, the properties of the wireless channel depend on the angular-dependent beam profiles of the transmitter and receiver, and their number. In the simulation, we only consider LOS propagation for the wireless channel. Reflected light in non-LOS propagation is usually weak, because most reflections are diffuse, unlike radio waves, where most reflections are specular. This is included in the channel model that has been developed and confirmed by measurements in [43].

To assess the properties of the communication link, we have derived formulas for the SNR-versus-frequency, including various combining techniques, the SVD and computed the achievable throughput. A 4 × 2 MIMO cell is evaluated in SDIV mode, and a 2 × 4 MIMO LIFi cell in SMUX mode, for selected user locations which were the same like in our measurements. The simulation framework is shown in Fig. 3.

B. EXPERIMENTAL SETUP

In the experimental setups for both SDIV and SMUX, POF was used to transmit the signals between CU and D-OFE as shown in Figs. 5 and 6. In both setups, the front-haul and the wireless units were similar as follows: The Avago transceiver AFBR-59F3Z was used for the bidirectional fronthaul transport over POF. At the transmission side, a 650 nm LED was used together with an integrated driver to convert the electrical signal into an optical signal. An integrated fiber-optical receiver with a PIN photo-diode and a trans-impedance amplifier (TIA) was used at the receiver. In the wireless link, the OFEs were equipped with off-the-shelf high-power LEDs operating at 860nm (OSRAM-SFH 4715 AS) and large-area silicon PDs (Hamamatsu S6968) as described in [44]. In the experiments, we employed the same OFEs both in the wireless infrastructure and at the mobile units.

The SDIV and SMUX modes were realized by using the real-time digital signal processing in a chipset supporting data transmission over several home networking media, i.e. coaxial cable, phone-line, power line, and POF, according to the ITU-T G.9960 home networking standard.

1) SDIV

The SDIV setup, as shown in Fig. 5, represents a 4×2 MIMO link. At the CU, we have used the Wave-2 DCP962P modem from Maxlinear in the coaxial cable mode. This modem is based on two chips, the 88LX5153 yields the digital baseband signals and the 88LX2730 provides the analog frontends output. We operated the CU as follows: In the downlink, the analog output CU signal of the digital baseband chip is replicated N_T times (number of OFEs) through Fanout buffers and sent

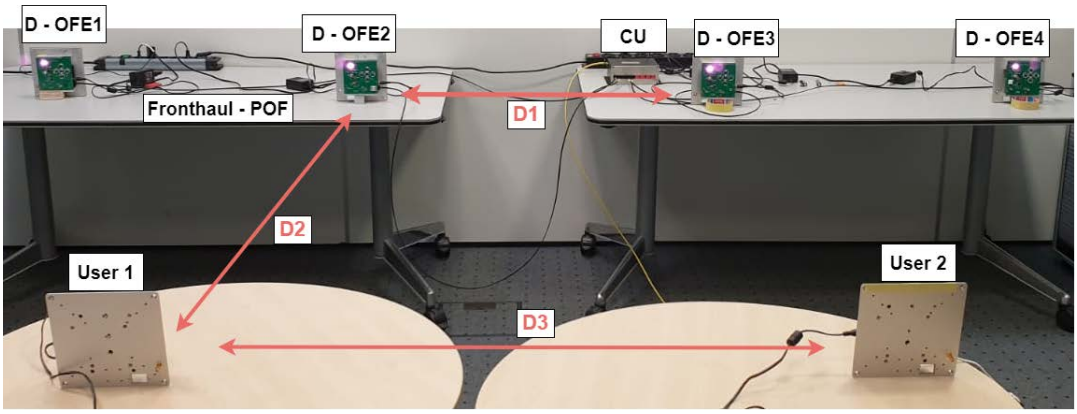

FIGURE 5. SDIV measurement setup. In the downlink, the CU distributes the signal equally and sends it via POF to D-OFEs. On the user side, there are two users with varying location. In the uplink, the CU combines the signals using either EGC or SC.

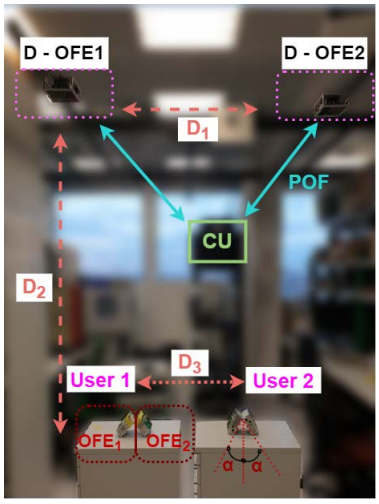

FIGURE 6. SMUX measurement setup. Each user is equipped with two OFEs [22].

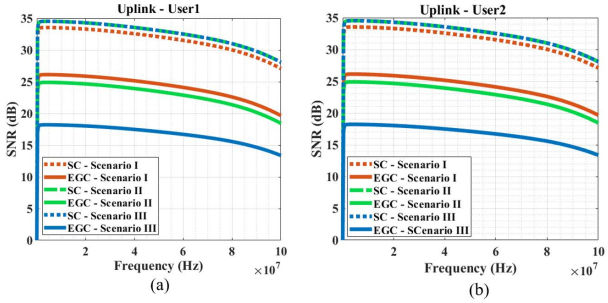

FIGURE 7. Simulated SNR vs. Frequency for up-link, including EGC as well as SC methods for user 1 (a) and user 2 (b), for the SDIV scenarios I, II, and III.

via the POF to each OFE from where it is transmitted over the wireless link and received by the MUs. In the uplink, the signals transmitted by the MUs are received by all OFEs, pre-amplified to compensate the loss when transmitting them over

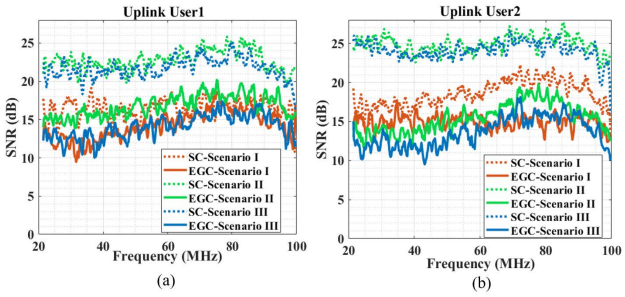

FIGURE 8. Measured SNR.vs Frequency for uplink, including EGC and SC methods for user 1 (a) and (b) user 2, for the SDIV scenarios I, II, and III.

the POF link. In the combiner, we can use either EGC or SC of all received signals. Both methods are implemented in the analog domain and hence, act identically on all sub-carriers of the DC-OFDM signal. Although this is theoretically sub-optimal, it works well in practice because optical propagation has a flat frequency response due to the LOS link and all OFEs have nearly identical responses. In SDIV mode, each MU has one OFE. All MUs are equipped with the same OFE also used in the D-OFE.

2) SMUX

The experimental setup for the SMUX link is shown in Fig. 6. The LiFi cell is defined as a 2×4 MIMO link, and the simulation emulates the same scenario as in the experiment. The CU was connected to two D-OFEs via POF. Each mobile device was equipped with two OFEs, which were either pointed into the same or different directions, indicated by the angle α. The CU was Maxlinear DCP962, operating in the phone-line mode, as defined in ITU-T recommendation G.9963 standard. The CU operated as a MIMO link with two channels connected via POF to each D-OFE. At the MU side, the OFEs were directly connected to the two channels of the same modem. This setup was also considered for evaluating the multi-user MIMO (MU-MIMO) performance. We observed

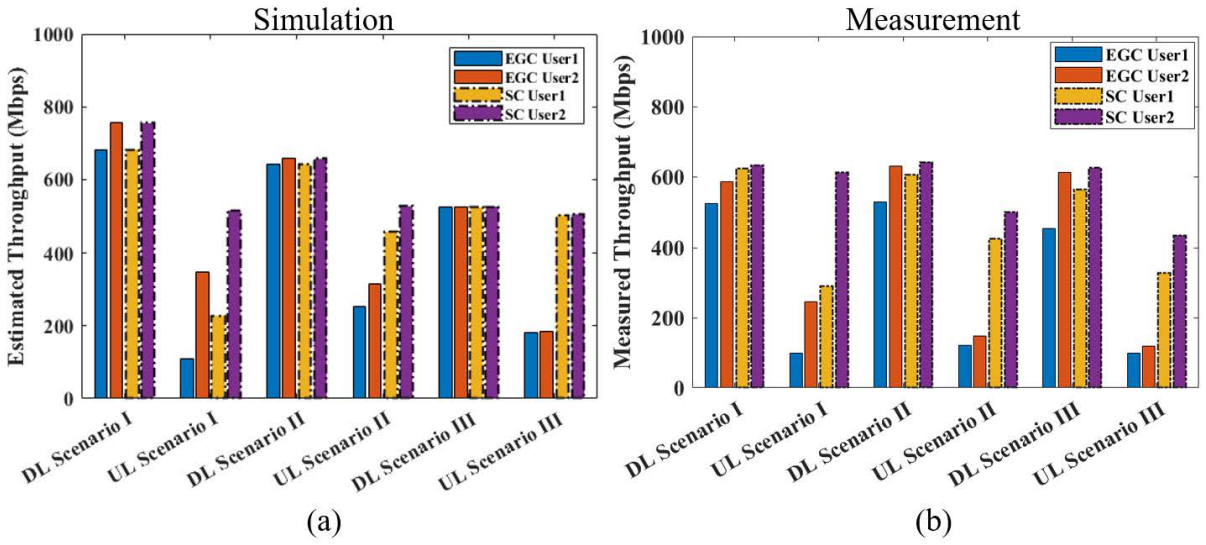

FIGURE 9. Throughput evaluation for different users locations considering both EGC and SC for downlink (DL) and uplink (UL).

that, after the modem was reset, it transmitted in multi-stream (MS) mode if the channel rank was high, and in single-stream (SS) mode if the channel rank was low. Thereby, the sum data rates in SS and MS modes can been directly measured or estimated for single user (SU) and MU-MIMO, based on the frequency-selective SNR measurements performed at both MU modems independently, following (21).

C. LiFi CELL LAYOUTS, SCENARIOS AND CASES

The LiFi cell layouts, scenarios and cases for SDIV and SMUX modes in the simulation and measurement are summarized in Table. 1. In both setups, D_1 is the distance between D-OFEs (same for all D-OFEs involved), D_2 the height of D-OFEs above MUs, and D_3 the distance of separation between two MUs. In each scenario, only D_3 was varied, and the other distances were kept constant.

V. RESULTS AND DISCUSSION

The following section presents the simulation and measurement results of both SDIV and SMUX modes, corresponding to the setups and scenarios introduced in section V-C.

A. SPATIAL DIVERSITY

In this subsection, the SDIV results are presented covering SNR and throughput.

1) SIGNAL-TO-NOISE -RATIO

At first, based on the model presented in section III-B, the SNR was simulated for EGC and SC for each scenario of each user, as shown in Fig. 7 (a,b). As mentioned before, the diversity combining was performed only in the uplink, while equal splitting was used in the downlink. Note that the SNR for both users were identical in the simulation, due to the symmetry in the scenarios and channel, accordingly. We observe that the SNR of SC always outperforms EGC in all scenarios. For instance, for user 1 in scenario I (Fig. 7(a), $D_3 = 5cm$, red line), where users were located close to each other, at 100 MHz the SNR of the EGC method is about 19 dB, while with SC it reaches approximately 27 dB. In scenario II ($D_3 = 90cm$, green line), user 1, by using EGC SNR at 100 MHz is about 18 dB, however, SC method leads to 27 dB, which is 50% enhancement of SNR. By using EGC, the received signals are summed with equal scaling, which leads to lower SNR for each user in comparison to SC method, where the received signals above a defined threshold are selected and summed. SC avoids adding the noise from the weak channel, which leads to a higher overall SNR. The same inspection for scenario III ($D_3 = 270cm$ blue-line) was observed by using SC method. The simulation results were principally confirmed by our experiments in the same scenarios, as shown in Fig. 8 (a,b). In the measurement, the SNR frequency spectrum was obtained with the monitoring software provided by the digital signal processor manufacturer [45]. SC improves only uplink SNR for both users, especially in scenarios II and III, e.g., for user 1 leads to 40% and 36.3% improvement, as shown by the green and blue dashed lines in Fig. 8 (a), respectively. SC is also effective in scenario I (dashed red lines of Fig. 7 (a,b)), but for instance, the SNR is only improved by about 3-5 dB, compared to full red line in Fig. 7 (b).

There are differences in the SNR values between the simulations and measurements. These differences are attributed to the empirical gap factor introduced in (21). It mainly takes the reduced modulation amplitude in real frontends into account to avoid clipping and non-linear distortion. In addition, there is always a penalty in real implementations, due to non-ideal coding and transmit signal shaping, which reduce the performance. Moreover, potential NLOS contributions were not included in our simulation analysis. Altogether, we observe that SC outperforms EGC significantly in terms of SNR.

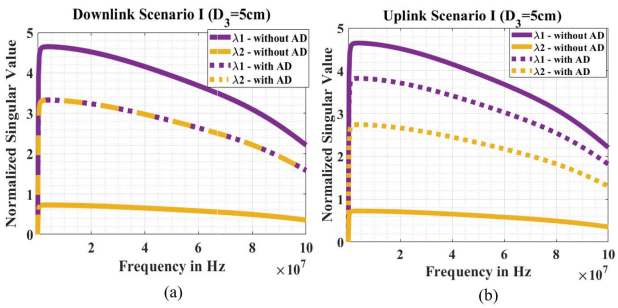

FIGURE 10. Simulation results for singular values in the SMUX cell layout described in Section V-C for D_3=5cm for two users without and with angular diversity for downlink (a) and uplink (b).

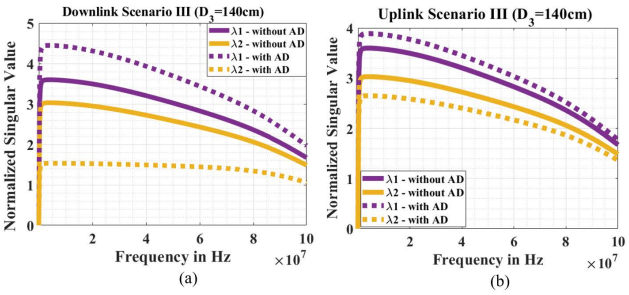

FIGURE 11. Simulation results for singular values in the SMUX cell layout described in Section V-C for D_3=140cm for two users without and with angular diversity for downlink (a) and uplink (b).

2) THROUGHPUT

The estimated and measured throughput for SDIV are shown in Fig. 9 (a,b). First of all, note that there is a difference between uplink and downlink performance, particularly when using EGC. This is due to the accumulation of noise when summing up four received signals. In addition, there are scenario-dependent differences, due to the different geometrical path gains depending on the user positions. In Fig. 9(a) the throughput is obtained by simulation from the SNR using (21). In the downlink, there are no differences between EGC and SC for each user, sequentially, as the signal simply replicated and sent to each D-OFE.

We observe that the simulated uplink throughput for each user is always higher when using SC compared to EGC. This is also confirmed by the measured throughput of each user obtained from the chipset software, as shown in Fig. 9 (b). SC leads to higher throughput for both users specifically in scenarios II and III. For instance, in uplink scenario III user 1, the throughput for the EGC mode (blue bar) is about 100 Mbps, while by SC mode (yellow bar) it increases to 328 Mbps.

B. SPATIAL MULTIPLEXING

Next, we consider SMUX by first assessing the singular values of the channel matrix in different scenarios and then by evaluating the throughput.

1) SINGULAR VALUES

Singular values are an indicator for the potential number of data streams that can be used in parallel for SMUX [46]. Besides, the singular values also show the potential amplitude gain in these parallel links. In the following, the singular value decomposition (SVD) of the MIMO channel matrix is evaluated through simulations for different SMUX scenarios following section (IV-C).

We consider the SMUX cell layout as shown in Fig. 3 (b) and Fig. 6, without and with AD. The singular values from simulations are shown for different spacing between the users, i.e. D_3= 5 cm in Fig. 10 and D_3= 140 cm in Fig.11. The SVD of user 1 and user 2 are denoted as λ_1 and λ_2. In the case of without AD, it is the continuous line and with AD it is the dashed line. If both users are nearby (scenario I) and have no AD, there is only one dominant singular value, i.e. only one of the users (see Fig. 9, λ_1 interprets as user1) can be served in the same time slot, both in downlink and uplink. If both users are nearby and AD is enabled, there are two dominant singular values. These singular values have about the same magnitude in the downlink but are somewhat different in the uplink. This attributes to non-reciprocity between uplink and downlink due to the different beam patterns of transmitter and receiver, which are typical for LiFi. When the distance between the users is larger (Scenario III), see Fig.11, also without AD can result in two dominant singular values.

Scenario II is similar to scenario III for both with and without AD. Therefore, we only show scenario III in Fig. 10. In the downlink (Fig. 10 (a)), there are two relatively equal singular values, when there is no AD (purple and yellow continuous line), indicating that the maximum capacity of the channel can be almost realized since the users are located far from each other and user have both OFEs pointing upwards. Introducing AD when users are far from each other, leads to unequal singular values, hence lower capacity. Considering the downlink direction in Fig. 5, OFE 1 of user 1 is not able to receive a strong signal, since it is looking away. But OFE 2 of user 1 can capture the strong signal from D-OFE 2. Therefore, λ_1, (purple dashed-line) has a higher value than λ_2 (yellow dashed-line). However, in the uplink (Fig. 10(b)), both singular values without and with AD have strong values. Altogether, AD leads to a more consistent behavior, specifically when users are close to each other, and uplink direction. Therefore, AD provides less dependency on the user positions in the cell. Despite being near to each other (scenario I), multiple data streams can be transmitted, as a benefit from AD.

2) THROUGHPUT

Throughput results for SMUX scenarios without and with AD and by using MU-MIMO were measured and evaluated, respectively. We consider MS transmission for each single user (SU). Results are shown in Fig. 12. We observe that the throughput is higher for all scenarios when using AD. In the scenario I, the gain due to AD is reduced, compared to other scenarios, because the link switched automatically to

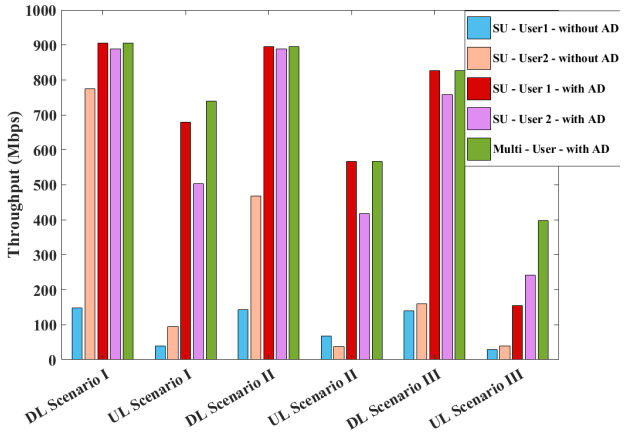

FIGURE 12. Measured throughput of spatial multiplexing in downlink and uplink for three defined scenarios and without and with angular diversity.

SS mode due to the short distance of the users to each other. MS results without AD are poor in general. When the channel matrix has reduced rank, it is harder to equalize the link using MS transmission mode.

At last, the value of multi-user multiplexing is evaluated. This is a more sophisticated mode, in which one stream is assigned to one user and the other stream to the other user. In MU-MIMO mode, each device receives the own data from the nearest OFE and suppresses the interference from the other stream which is assigned to the other device. Note that both devices employ their MIMO equalizers, therefore, i.e. the other data stream is separated from the own stream, but it is not decoded and discarded at the interface to the medium access layer. In this way, we can theoretically combine the highest fractional rates from both users to evaluate the value of MU-MIMO, which is shown as green bars in Fig. 12. We observe that in the downlink, MU multiplexing does not enhance the throughput in the scenarios investigated here. But in the uplink, communication is more limited by the noise, and then the combination of signals from two users become efficient. For instance, in Scenarios I and III (uplink) we observe that the throughput increases by combining the best streams. These results indicate that multi-user multiplexing has always the highest performance, which is sometimes also reached by combining the streams from the same user. Nonetheless, our measurements show that having the option of combining streams for different users in one MIMO link can lead to the same or eventually higher throughput.

VI. CONCLUSION

In this paper, we presented for the first time an all-optical distributed wireless communication system for future IIoT applications and tested it in real-time by using the ITU-T G.9991 standard. For implementing the fronthaul, we used plastic optical fiber to distribute the signals from the central unit to the distributed optical frontends. Next, these signals were transmitted through the optical wireless link to each mobile user. To analyze the proposed system, a theoretical signal model was developed, which allows for evaluating the performance of the concatenated wired and wireless links. The system was considered as a distributed multiple-input multiple-output link that can be operated in different transmission modes: spatial diversity and spatial multiplexing. We investigated the performance of these modes by means of simulation and measurements in different scenarios. We observed that the performance of each transmission mode highly depends on the channel condition, besides the received power. Both are related to the spacing between the users and the distance to the OFEs. Moreover, for closely-spaced users, SDIV enables better performance than SMUX without angular diversity. Selection combining provides impressive diversity gains over equal gain combining, which is attributed to the spatial selectivity of the optical wireless channel. We have also considered SMUX in combination with angular diversity, which improves the performance depending on the user location. In low SNR scenarios, specifically in the uplink, we observed that multi-user multiplexing can achieve additional gains. As an outlook, future work need to consider dynamic switching between these spatial transmission modes, i.e. single- and multi-stream transmission for single and multiple users, to maximize the performance in each scenario. Channel estimation for distributed MIMO, the required feedback and control loop are defined in the upcoming IEEE standard 802.15.13 for LiFi. This will enable setups with more distributed optical frontends and a larger statistics when users are mobile.

REFERENCES

[1] N. Chi, Y. Zhou, Y. Wei, and F. Hu, "Visible light communication in 6G: Advances, challenges, and prospects," *IEEE Veh. Technol. Mag.*, vol. 15, no. 4, pp. 93–102, Dec. 2020.
[2] V. Jungnickel, P. W. Berenguer, S. M. Mana, M. Hinrichs, S. M. Kouhini, K. L. Bober, and C. Kottke, "LiFi for industrial wireless applications," in *Proc. Opt. Fiber Commun. Conf. Exhib. (OFC)*, 2020, pp. 1–3.
[3] L. Grobe, A. Paraskevopoulos, J. Hilt, D. Schulz, F. Lassak, F. Hartlieb, C. Kottke, V. Jungnickel, and K. Langer, "High-speed visible light communication systems," *IEEE Commun. Mag.*, vol. 51, no. 11, pp. 60–66, Dec. 2013.
[4] G. L. Stüber, J. R. Barry, S. W. McLaughlin, Y. Li, M. A. Ingram, and T. G. Pratt, "Broadband MIMO-OFDM wireless communications," *Proc. IEEE*, vol. 92, no. 2, pp. 271–294, Feb. 2004.
[5] K. L. Bober, S. M. Mana, M. Hinrichs, S. M. Kouhini, C. Kottke, D. Schulz, C. Schmidt, R. Freund, and V. Jungnickel, "Distributed multiuser MIMO for LiFi in industrial wireless applications," *J. Lightw. Technol.*, vol. 39, no. 11, pp. 3420–3433, Jun. 2021.
[6] M. Aazam, S. Zeadally, and K. A. Harras, "Deploying fog computing in industrial Internet of Things and industry 4.0," *IEEE Trans. Ind. Informat.*, vol. 14, no. 10, pp. 4674–4682, Oct. 2018.
[7] D. Tse and P. Viswanath, *Fundamentals of Wireless Communication*. Cambridge, U.K.: Cambridge Univ. Press, 2005.
[8] C. Chen, W.-D. Zhong, and D. Wu, "On the coverage of multiple-input multiple-output visible light communications," *J. Opt. Commun. Netw.*, vol. 9, no. 9, pp. D31–D41, 2017.
[9] P. W. Berenguer, D. Schulz, J. Hilt, P. Hellwig, G. Kleinpeter, J. K. Fischer, and V. Jungnickel, "Optical wireless MIMO experiments in an industrial environment," *IEEE J. Sel. Areas Commun.*, vol. 36, no. 1, pp. 185–193, Jan. 2018.
[10] S. M. Mana, V. Jungnickel, K. L. Bober, P. Hellwig, J. Hilt, D. Schulz, A. Paraskevopoulos, R. Freund, K. Hirmanova, R. Janca, P. Chvojka, and S. Zvanovec, "Distributed multiuser MIMO for LiFi: Experiments in an operating room," *J. Lightw. Technol.*, vol. 39, no. 18, pp. 5730–5743, Sep. 2021.

[11] T. Fath and H. Haas, "Performance comparison of MIMO techniques for optical wireless communications in indoor environments," *IEEE Trans. Commun.*, vol. 61, no. 2, pp. 733–742, Feb. 2013.

[12] C. Chen, H. Yang, P. Du, W.-D. Zhong, A. Alphones, Y. Yang, and X. Deng, "User-centric MIMO techniques for indoor visible light communication systems," *IEEE Syst. J.*, vol. 14, no. 3, pp. 3202–3213, Sep. 2020.

[13] T. A. Tsiftsis, H. G. Sandalidis, G. K. Karagiannidis, and M. Uysal, "Optical wireless links with spatial diversity over strong atmospheric turbulence channels," *IEEE Trans. Wireless Commun.*, vol. 8, no. 2, pp. 951–957, Feb. 2009.

[14] T. Song, A. Nirmalathas, C. Lim, E. Wong, K.-L. Lee, Y. Hong, K. Alameh, and K. Wang, "Performance analysis of repetition-coding and space-time-block-coding as transmitter diversity schemes for indoor optical wireless communications," *J. Lightw. Technol.*, vol. 37, no. 20, pp. 5170–5177, Oct. 2019.

[15] P. W. Berenguer, P. Hellwig, D. Schulz, J. Hilt, G. Kleinpeter, J. K. Fischer, and V. Jungnickel, "Real-time optical wireless mobile communication with high physical layer reliability," *J. Lightw. Technol.*, vol. 37, no. 6, pp. 1638–1646, Mar. 15, 2019.

[16] Y. Bian, X. Cheng, M. Wen, L. Yang, H. V. Poor, and B. Jiao, "Differential spatial modulation," *IEEE Trans. Veh. Technol.*, vol. 64, no. 7, pp. 3262–3268, Jul. 2015.

[17] X. Zhu, Z. Wang, Q. Wang, and H. Haas, "Virtual spatial modulation for MIMO systems," in *Proc. IEEE Global Commun. Conf. (GLOBECOM)*, Dec. 2016, pp. 1–6.

[18] R. Y. Mesleh, H. Haas, S. Sinanovic, C. W. Ahn, and S. Yun, "Spatial modulation," *IEEE Trans. Veh. Technol.*, vol. 57, no. 4, pp. 2228–2241, Jul. 2008.

[19] X. Zhong, C. Chen, S. Fu, X. Jian, and M. Liu, "Generalized spatial multiplexing for optical wireless communication systems," in *Proc. 12th Int. Conf. Adv. Infocomm Technol. (ICAIT)*, Nov. 2020, pp. 23–27.

[20] T. Song, C. Lim, A. Nirmalathas, and K. Wang, "Optical wireless communications using signal space diversity with spatial modulation," *Photonics*, vol. 8, no. 11, p. 468, 2021.

[21] I. Tavakkolnia, M. D. Soltani, M. A. Arfaoui, A. Ghrayeb, C. Assi, M. Safari, and H. Haas, "MIMO system with multi-directional receiver in optical wireless communications," in *Proc. IEEE Int. Conf. Commun. Workshops (ICC Workshops)*, May 2019, pp. 1–6.

[22] S. Kouhini, P. Hellwig, D. Schultz, R. Freund, and V. Jungnickel, "Benefits of MIMO mode switching, angular diversity and multiuser multiplexing for LiFi," in *Proc. Opt. Fiber Commun. Conf.* Washington, DC, USA: Optical Society of America, 2021, pp. 1–3, Paper F1A-7.

[23] S. M. Kouhini, S. M. Mana, R. Freund, V. Jungnickel, C. R. B. Corrêa, E. Tangdiongga, T. Cunha, X. Deng, and J.-P. M. Linnartz, "Distributed MIMO experiment using LiFi over plastic optical fiber," in *Proc. IEEE Globecom Workshops (GC Wkshps)*, Dec. 2020, pp. 1–6.

[24] I. C. Sezgin, T. Eriksson, J. Gustavsson, and C. Fager, "Evaluation of distributed MIMO communication using a low-complexity sigma-delta-over-fiber testbed," in *IEEE MTT-S Int. Microw. Symp. Dig.*, Jun. 2019, pp. 754–757.

[25] S. Ma, Y. Yang, and H. Sharif, "Distributed MIMO technologies in cooperative wireless networks," *IEEE Commun. Mag.*, vol. 49, no. 5, pp. 78–82, May 2011.

[26] P. W. Berenguer, D. Schulz, J. K. Fischer, and V. Jungnickel, "Distributed 8×6 MIMO experiments for optical wireless communications," in *Proc. Eur. Conf. Opt. Commun. (ECOC)*, 2017, pp. 1–3.

[27] S. M. Mana, S. M. Kouhini, P. Hellwig, J. Hilt, P. W. Berenguer, and V. Jungnickel, "Distributed MIMO experiments for LiFi in a conference room," in *Proc. 12th Int. Symp. Commun. Syst., Netw. Digit. Signal Process. (CSNDSP)*, 2020, pp. 1–5.

[28] K.-S. Hwang, Y.-C. Ko, and M.-S. Alouini, "Outage probability of cooperative diversity systems with opportunistic relaying based on decode-and-forward," *IEEE Trans. Wireless Commun.*, vol. 7, no. 12, pp. 5100–5107, Dec. 2008.

[29] S. M. Kouhini, S. M. Mana, P. Hellwig, J. Hilt, D. Schulz, A. Paraskevopoulos, R. Freund, and V. Jungnickel, "Performance of bidirectional LiFi over plastic optical fiber (POF)," in *Proc. 12th Int. Symp. Commun. Syst., Netw. Digit. Signal Process. (CSNDSP)*, Jul. 2020, pp. 1–6.

[30] A. Checko, H. L. Christiansen, Y. Yan, L. Scolari, G. Kardaras, M. S. Berger, and L. Dittmann, "Cloud ran for mobile networks—A technology overview," *IEEE Commun. Surveys Tuts.*, vol. 17, no. 1, pp. 405–426, 1st Quart., 2014.

[31] A. Nuwanpriya, S.-W. Ho, and C. S. Chen, "Angle diversity receiver for indoor MIMO visible light communications," in *Proc. IEEE Globecom Workshops (GC Wkshps)*, Dec. 2014, pp. 444–449.

[32] Z. Chen, N. Serafimovski, and H. Haas, "Angle diversity for an indoor cellular visible light communication system," in *Proc. IEEE 79th Veh. Technol. Conf. (VTC Spring)*, May 2014, pp. 1–5.

[33] J. M. Kahn and J. R. Barry, "Wireless infrared communications," *Proc. IEEE*, vol. 85, no. 2, pp. 265–298, Feb. 1997.

[34] P. W. Berenguer, J. Hilt, P. Hellwig, D. Schulz, J. K. Fischer, and V. Jungnickel, "Analog antenna diversity for reliable optical wireless communication systems," in *Proc. Global LIFI Congr. (GLC)*, Feb. 2018, pp. 1–5.

[35] Y. Tan and H. Haas, "Coherent LiFi system with spatial multiplexing," *IEEE Trans. Commun.*, vol. 69, no. 7, pp. 4632–4643, Jul. 2021.

[36] A. Mohamed, A. H. Zekry, and R. Ibrahim, "FPGA implementation of sphere detector for spatial multiplexing MIMO system," *Int. J. Electron. Telecommun.*, vol. 65, 2019.

[37] V. Jungnickel, S. Jaeckel, L. Thiele, L. Jiang, U. Kruger, A. Brylka, and C. Von Helmolt, "Capacity measurements in a cooperative MIMO network," *IEEE Trans. Veh. Technol.*, vol. 58, no. 5, pp. 2392–2405, Jun. 2009.

[38] W. A. Shehab and Z. Al-Qudah, "Singular value decomposition: Principles and applications in multiple input multiple output communication system," *Int. J. Comput. Netw. Commun.*, vol. 9, no. 1, pp. 13–21, 2017.

[39] E. Biglieri *et al.*, *MIMO Wireless Communications*. Cambridge, U.K.: Cambridge Univ. Press, 2007.

[40] D. Tse and P. Viswanath, *Fundamentals of Wireless Communication*. Cambridge, U.K.: Cambridge Univ. Press, 2005.

[41] G. J. Foschini and M. J. Gans, "On limits of wireless communications in a fading environment when using multiple antennas," *Wireless Pers. Commun.*, vol. 6, no. 3, pp. 311–335, Mar. 1998.

[42] S. Mardanikorani, X. Deng, and J.-P. M. G. Linnartz, "Sub-carrier loading strategies for DCO-OFDM LED communication," *IEEE Trans. Commun.*, vol. 68, no. 2, pp. 1101–1117, Feb. 2020.

[43] S. M. Mana, K. G. Gabra, S. M. Kouhini, M. Hinrichs, D. Schulz, P. Hellwig, A. Paraskevopoulos, R. Freund, and V. Jungnickel, "LiDAR-assisted channel modelling for LiFi in realistic indoor scenarios," *IEEE Access*, vol. 10, pp. 59383–59399, 2022.

[44] S. M. Kouhini, E. A. Jarchlo, R. Ferreira, S. Khademi, G. Maierbacher, B. Siessegger, D. Schulz, J. Hilt, P. Hellwig, and V. Jungnickel, "Use of plastic optical fibers for distributed MIMO in Li-Fi systems," in *Proc. Global LIFI Congr. (GLC)*, Jun. 2019, pp. 1–5.

[45] MaxLinear. (2019). *Wave-2 Coax and Phone Line Networking Evaluation*. [Online]. Available: https://www.mouser.de/datasheet/2/146/wave-2-coaxial-and-phone-line-networking-evaluatio-1815047.pdf

[46] D. Tse and P. Viswanath, "MIMO I: Spatial multiplexing and channel modeling," in *Fundamentals of Wireless Communication*. 2005, pp. 290–331.

SEPIDEH MOHAMMADI KOUHINI (Graduate Student Member, IEEE) received the B.S. degree in electronic engineering from Azad University and the M.S. degree in electronic engineering from ACECR University, Iran. She has been with the Fraunhofer Heinrich Hertz Institute (HHI), since 2019. She is currently a Ph.D. Researcher with TU Berlin University. She is also working on 6G-RIC Project with Fraunhofer HHI. She has participated in several national and international projects in universities and research institutes such as APIC and VisIon at the Institute Telecommunication of Aveiro, OSRAM Innovation Garching-Munich. Her research interests include optical wireless communications and localization.

JULIAN HOHMANN received the M.Eng. degree in electrical engineering from the Berlin University of Applied Sciences, Berlin, Germany, in 2017. Since 2014, he has been with the Department of Photonic Networks and Systems, Fraunhofer Institute for Telecommunications, Heinrich Hertz Institute, Berlin, where he is currently an Electrical Engineer. His current research interests include design, realization, and test of optical wireless communication systems.

SREELAL MAVANCHERY MANA received the M.Tech. degree in optical engineering from the Indian Institute of Space Science and Technology, Thiruvananthapuram, India, in 2017. He is currently pursuing the Ph.D. degree in optical wireless communications. Since August 2018, he has been a Marie-Curie Research Fellow with the Department of Photonic Networks and Systems, Fraunhofer Institute for Telecommunications, Heinrich Hertz Institute, Berlin, Germany. His current research interests include channel modeling simulation and experiments for optical wireless communication systems, MU MIMO for LiFi networks, and DCO-OFDM systems.

PETER HELLWIG received the Diploma degree in electrical engineering from the Berlin University of Applied Sciences, Berlin, Germany, in 2009. In 2016, he joined the Fraunhofer Institute for Telecommunications, Heinrich Hertz Institute, where he is currently working as an Electrical Engineer with the Department of Photonic Networks and Systems. His current research interests include design and realization of visible light communication systems.

DOMINIC SCHULZ received the M.Eng. degree in communications engineering from the Berlin University of Applied Sciences, Berlin, Germany, in 2012, and the Ph.D. degree from the Technical University of Berlin, Berlin, in 2019. In 2012, he joined the Department of Photonic Networks and Systems, Fraunhofer Institute for Telecommunications, Heinrich Hertz Institute, Berlin, where he is currently working in the field of optical wireless communications. His current research interests include development of high data rate systems for wireless access and research towards short-range outdoor backhaul links for small radio cells and wireless-to-the-home.

ANAGNOSTIS PARASKEVOPOULOS (Member, IEEE) received the degree in electrical engineering from the Technical University of Athens and the Ph.D. degree from Université Paris-Orsay with a study on RF modulation of semiconductor lasers performed in CNET, Research Centre France Telecom, Paris. He joined HHI, in 1988, and was since involved in various research projects, including the ESPRIT263 Project on HBTs and the National Project on VCSEL devices at 980 nm in the early 90's and custom designed laser diodes for non-telecom applications. Over the years, he has successfully coordinated Research and Development projects, concerning both research subjects and industrial applications. He is the author and the coauthor of more than 50 scientific papers. His current research interest includes applications for optical wireless communication and LiFi.

RONALD FREUND (Member, IEEE) received the Dipl.-Ing. and Dr.-Ing. degrees in electrical engineering from the Technical University of Ilmenau, Ilmenau, Germany, in 1993 and 2002, respectively, and the M.B.A. degree from RWTH Aachen University, Aachen, Germany. In 1997, he co-founded VPI Systems Inc., where he was the Chief Technology Officer and a Consultant, responsible for the development of design software for the physical layer of photonic networks. In 2017, he was appointed as a Professor of photonic communication systems with the Technical University of Berlin, Berlin, Germany. Since 1995, he has been with the Heinrich Hertz Institute, Berlin, where he is currently leading the Department of Photonic Networks and Systems. He has authored or coauthored more than 150 scientific publications.

VOLKER JUNGNICKEL (Member, IEEE) received the Ph.D. degree in physics and communications engineering from Humboldt University, Berlin, in 1995, and the Habilitation degree in physics and communications engineering from Technical University, Berlin, in 2015. He joined Fraunhofer HHI, in 1997, where he is currently working on optical wireless communication, adaptive multiple antenna techniques in mobile networks, and fixed optical access infrastructures. Besides, he serves at Technical University as a Privatdozent, where he teaches courses on advanced wireless communications and supervising master's and Ph.D. thesis. He serves as the Chair for IEEE P802.15.13 Task Group on Multi-Gbit/s Optical Wireless Communications and the Technical Editor for the IEEE P802.11bb Task Group on Light Communications.